Chinese Chemical Letters 34 (2023) 108092

Contents lists available at ScienceDirect

Chinese Chemical Letters

journal homepage: www.elsevier.com/locate/cclet

A novel cartridge for nucleic acid extraction, amplification and detection of infectious disease pathogens with the help of magnetic nanoparticles

Yile Fang[a], Yue Wang[a], Liangxi Zhu[a], Haoran Liu[a], Xiangyi Su[a], Yuan Liu[a], Zhu Chen[b], Hui Chen[b], Nongyue He[a,b,*]

[a] State Key Laboratory of Bioelectronics, School of Biological Science and Medical Engineering, Southeast University, Nanjing 210096, China
[b] Economical Forest Cultivation and Utilization of 2011 Collaborative Innovation Center in Hunan Province, Hunan Key Laboratory of Green Chemistry and Application of Biological Nanotechnology, Hunan University of Technology, Zhuzhou 412007, China

ARTICLE INFO

Article history:
Received 17 October 2022
Revised 20 December 2022
Accepted 21 December 2022
Available online 24 December 2022

Keywords:
Nucleic acid detection
Cartridge
Magnetic nanoparticles
Fluidic control
Point-of-care testing

ABSTRACT

Nucleic acid detection (NAD) based on real-time polymerase chain reaction (real-time PCR) is gold standard for infectious disease detection. Magnetic nanoparticles (MNPs) are widely used for nucleic acid extraction (NAE) because of their excellent properties. Microfluidic technology makes automated NAD possible. However, most of the NAD microfluidic chips are too complex to be applied to point-of-care (POC) testing. In this paper, a simple-structure cartridge was developed for POC detection of infectious diseases. This self-contained cartridge can be divided into a magnetic-controlled NAE part, a valve-piston combined fluidic control part and a PCR chip, which is able to extract nucleic acid from up to 500 μL of liquid samples by MNPs and finish the detection process from "sample in" to "answer out" automatically. Performance tests of the cartridges show that it met the demands of automated NAD. Results of on-cartridge detection of hepatitis B virus (HBV) demonstrated that this system has good uniformity and no cross-contamination between different cartridges, and the limit of detection (LOD) of this system for HBV in serum is 50 IU/mL. Multiplex detections of severe acute respiratory syndrome coronaviruses 2 (SARS-CoV-2) with a concentration of 500 copies/mL were carried out on the system and 100% positive detection rate was achieved.

Since the 21th century, there have been frequent outbreak of infectious diseases such as severe acute respiratory syndrome (SARS), Middle East respiratory syndrome (MERS) [1], Zika and Ebola [2,3]. Especially the current corona virus disease 2019 (COVID-19) caused by severe acute respiratory syndrome coronavirus 2 (SARS-CoV-2) has become the most serious challenge in the world [4,5]. In the past two years, a large number of detection methods have been developed for the rapid detection of SARS-CoV-2, such as recombinase polymerase amplification (RPA) [6], loop-mediated isothermal amplification (LAMP) [7], antigen-based detection methods [8], as well as CRISRP-based methods [9,10]. However, these methods still have shortcomings in terms of accuracy and sensitivity. Reverse transcription real-time polymerase chain reaction (RT real-time PCR) is still the gold standard for detecting SARS-CoV-2 [11,12]. However, most of the current mainstream nucleic acid detection (NAD) kits are applied for sample processing, amplification and detection step by step, which involve a lot of manual operations and require a laboratory environment as well as various of equipment. Too many manual operations will increase the risk of cross-contamination, which may lead to false test results. In order to solve these shortcomings, many research teams have developed integrated NAD devices based on microfluidic chips to automatically realize "sample-in to result out", greatly improving the efficiency of NAD [13–19]. For example, Huang *et al.* developed a microfluidic chip-based PCR-array system to complete the detection of 21 pathogens in a fully integrated manner [20]. The system used a microfluidic chip packaged with all the reagents required, and sample lysis, nucleic acid extraction/purification and real-time PCR are sequentially implemented on the same chip. Zong *et al.* presented an automated centrifugal microfluidic chip to achieve hepatitis B virus (HBV) genotyping from whole blood only in about 1 h [21]. Li *et al.* constructed a self-contained fluidic cassette for multiplex detection of bacteria for rapid diagnosis of urinary tract infections [22]. The kit was successfully applied to detect four ma-

* Corresponding author.
E-mail address: nyhe1958@163.com (N. He).

https://doi.org/10.1016/j.cclet.2022.108092
1001-8417/

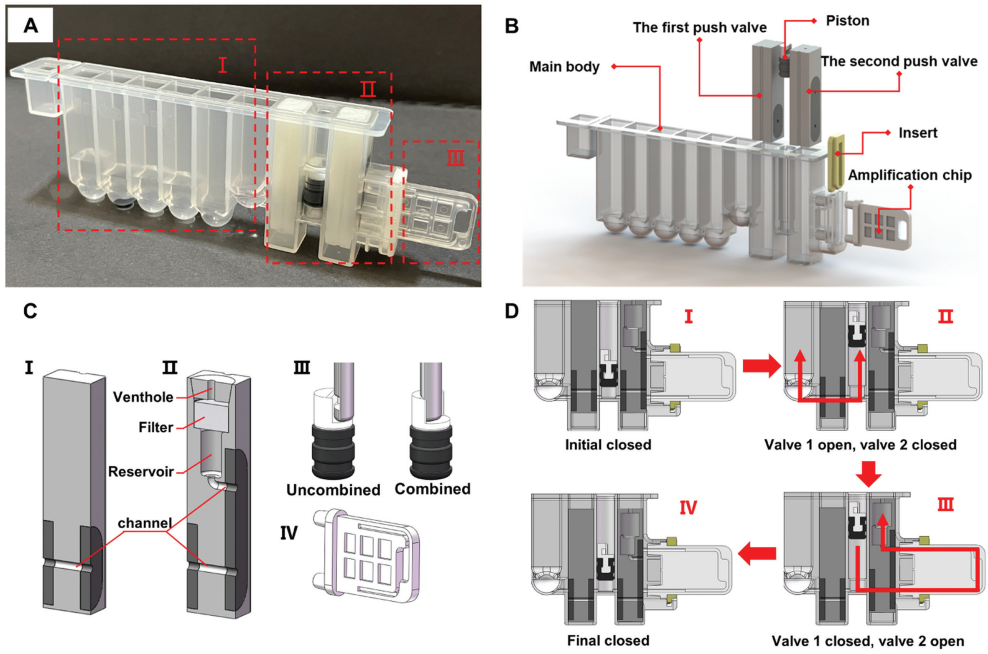

Fig. 1. Schematic of the integrated cartridge. (A) Photo of the cartridge, which can be divided into three parts: (I) the magnetic-controlled NAE part, (II) the valve-piston combined fluidic control part and (III) the PCR chip; (B) The 3D illustration of the cartridge in an exploded view; (C) Detailed structure of the cartridge components, (I) sectional view of the first push valve, (II) sectional view of the second push valve, (III) combination status of the piston and the control lever, (IV) the structure of the PCR chip; (D) The principle of valve-piston combined fluidic control.

jor pathogenic bacteria in Urinary tract infections (UTIs). Trick *et al.* developed an imaging-based portable droplet magneto-fluidic cartridge platform, which can detect multiple SARS-CoV-2 variants or other respiratory pathogens [23].

In summary, most of the microfluidic chip-based integrated NAD devices reported so far contain complex structures of flow channels and chambers, or require additional pumps or valves for precise fluidic control, which will undoubtedly increase the manufacturing difficulty and use cost [24,25]. On the other hand, due to size constraints, the microfluidic chips can only handle a few tens of microliters or even a few microliters of sample, which will greatly reduce the sensitivity of the assay and easily cause false-negative results at low sample concentrations [26,27].

Based on the previous work of our research group [28–31], in this paper, an integrated cartridge with simple structure was developed for automatic nucleic acid extraction (NAE), amplification and fluorescence detection. The current simple-structure cartridge only has six components and can be divided into three functional parts of magnetic-controlled NAE part, valve-piston combined fluidic control part and a PCR chip. The NAE part can process up to 500 μL of liquid samples, and quickly complete nucleic acid processing step in 10 min. All reagents required for detection are preloaded into the appropriate wells, after loading the sample, the whole workflow including sample lysis, nucleic acid binding to magnetic nanoparticles (MNPs), washing, nucleic acid elution, mixing the nucleic acid template with amplification reagents, distributing the mixture into the chip, and real-time PCR, is automatically executed. This simple-structure and easy-to-use cartridge system is suitable for point-of-care (POC) testing of various infectious disease pathogens.

Performance evaluations of this system have been conducted, and the results demonstrated that the designed cartridge was good at magnetic control and fluidic control, and on-cartridge NAE had better efficiency than manual extraction which involved multiple centrifugation steps. In addition, the four cartridge channels in the device have good uniformity and there is no cross-contamination between cartridges. The limit of detection (LOD) of this system for HBV in serum is 50 IU/mL. Multiplex detections of severe acute respiratory syndrome coronaviruses 2 (SARS-CoV-2) with a concentration of 500 copies/mL were carried out on the system and 100% positive detection rate was achieved.

Magnetic nanoparticles (MNPs) are new materials with rapid development and great application value in many fields of modern science [32]. In the cartridge, MNPs based NAE was chose to extract and purify nucleic acids from samples to be tested for downstream detection. Fig. S1 (Supporting information) shows the schematic diagram of the NAE, in which a magnetic rod as well as a magnetic rod sleeve were cooperated with each other to complete the operation of mixing, adsorption and transfer of the MNPs.

Depending on the function, the integrated cartridge (11.5 cm × 3.5 cm × 1.5 cm) can be divided into three parts (Fig. 1A): (I) the magnetic-controlled NAE part, (II) the valve-piston combined fluidic control part and (III) the PCR chip. The exploded view of the cartridge (Fig. 1B) indicates that the simple-structure cartridge only consists of six components: the main body of the cartridge, two push valves, a piston, an insert and a PCR chip. The main body and the body of the PCR chip were injection molded by Shenzhen KK Medical Technology Co., Ltd. (Shenzhen, China). Two pressure-sensitive adhesive films (ARseal 90697, Adhesives Research China Co., Ltd.) are covered on both sides of the chip. Apart from the main body and the PCR chip, other components were manufactured by three-dimensional (3D) printing.

Fig. 1C further shows detailed of the cartridge components. The sectional view shows the internal structure of the two push valves. As we can see, both valves have a channel passing through the valve body in a lower position. Besides, the second push valve has a second channel in a higher position connecting with a reservoir. A filter is installed between the reservoir and the venthole, which can prevent the aerosol escaping into the air. To improve the sealing of the valves, we set flexible silicone pads around the channel to ensure a tight fit between the valve and the main body of the cartridge. To realize push and pull actions of the piston, we de-

signed a complementary structure for the piston and the control lever so that they can combine and separate automatically. When combined with the piston, the control lever can pull and push the piston to pump the liquid in and out. The PCR chip which contains a reaction chamber (30 μL) and two channels was designed to be flattened to improve heat transfer efficiency. The two channels of the chip are match for the channels on the second push valve so that the PCR reagents can be pumped into the chip through the push valve. Fig. 1D indicates the principle of valve-piston combined fluidic control: (I) The two push valves are initial closed and the piston is at the bottom of the well; (II) The first valve is pushed down to open, then the piston can pump the liquid in and out through the first valve; (III) The first valve is pushed down again to close while the second valve is pushed down to open, then the piston can pump the mixed reagents into the PCR chip; (IV) The second valve is pushed down again to close to form a sealed environment for PCR.

The cartridge system proposed in this work is designed for "sample-in to answer-out" NAD of infectious disease pathogens. The reagents and detection processes may be slightly different for different kinds of samples. A typical workflow of the cartridge including nine steps in total is demonstrated in Fig. S2 (Supporting information), of which only the first step needs manual operation. All required reagents have been preloaded into the appropriate wells, and a specific arrangement of the reagents loading is: 400 μL of lysis & binding buffer in the well 1#, 20 μL of MNPs with 400 μL of pure water in the well 2#, 500 μL of washing buffer I in the well 3#, 500 μL of washing buffer II in the well 4#, 80 μL of elution buffer in the well 6# and 40 μL of PCR mixture in the piston well. Detailed procedure can be found in Supporting information.

After completing the construction of the cartridge system, a series of validation experiments were conducted to evaluate the performance of the system. The reagents and samples used in the validation experiments are listed in Supporting information.

A series of performance tests of the designed cartridge were carried out for evaluating whether it could meet the demands of NAD. First, the operation of mixing, adsorption and transfer of MNPs in the cartridge were tested. Three liquid systems with total volumes of 500 μL (300 μL lysis buffer and 200 μL serum samples), 700 μL (400 μL lysis buffer and 300 μL serum samples) and 1000 μL (500 μL lysis buffer and 500 μL serum samples) were set up and 20 μL of MNPs were added to each system and gathered to the bottom of the tube by a magnet. Then, cartridges with the set-up liquid systems were loaded to the device and the magnetic rod sleeve mixed the liquid system by vibrating up and down at high speed (6 times per second) for 30 times. For different volumes, the oscillation amplitude of the magnetic rod sleeve will be adjusted to adapt the liquid level. Fig. 2A shows the comparison image of before and after mixing of the MNPs, indicating that the magnetic sleeve had excellent mixing effect on the MNPs in both large and small volume liquid systems. Besides, Fig. 2B shows the comparison image of before and after transferring MNPs from well 1# to well 3#. As we can see, after completing the transfer, no MNPs remained in well 1# while the beads transferred to well 3# could restore uniform suspension state easily.

After that, fluid control performance of the cartridge was tested. Firstly, the ability to dissolve the lyophilized PCR reagents was tested. As shown in Fig. 2C, before dissolution, elution buffer was in well 6# while the lyophilized PCR reagent was in the piston well. To begin the dissolution, the first push valve was pressed down to open the channel, and then the piston was moved up and down 5 times to drive the liquid in-and-out of the piston well repeatedly to fully dissolve the lyophilized PCR reagent in the piston tube. Fig. 2D shows the workflow of transferring reagents from well 6# to PCR chip: (I) The reagents were in well 6# and the two

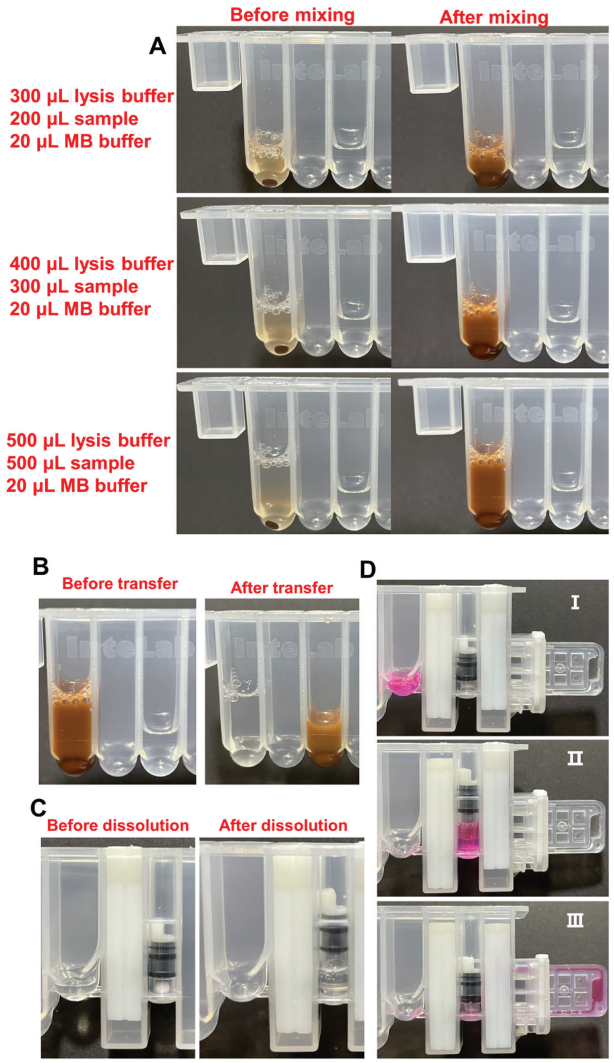

Fig. 2. Images of performance evaluation results of the cartridge. (A) Comparison of before and after mixing of MNPs at different volumes of samples. (B) Comparison of before and after transferring MNPs from well 1# to well 3#. (C) Comparison of before and after dissolving lyophilized PCR reagents under control of the piston and the push valve. (D) Workflow of transferring reagents from well 6# to PCR chip: (I) The reagents were in well 6#; (II) piston aspirated the reagents with the cooperation of the first push valve; (III) piston injected the reagents into PCR chip with the cooperation of the second valve.

push valves were closed; (II) The first push valve was pressed to open the first channel and the piston was lifted upwards to absorbed the reagents into the piston well; (III) The first push valve was pressed again to close the first channel while the second push valve was pressed to open the second channel and then the piston was pressed down to injected the reagents into PCR chip.

Four groups of serum samples containing HBV at concentrations of 5×10^3 IU/mL, 5×10^4 IU/mL, 5×10^5 IU/mL, and 5×10^6 IU/mL were selected, and 200 μL of each sample were extracted manually and automatically by this cartridge system. To increase comparability, the steps for manual extraction are the same as those for automatic extraction. After that, the purified samples were amplified and detected using the StepOnePlus Real-time PCR System (Applied Biosystems, America). Figs. 3A and B indicate the real-time PCR results comparison of the two extraction methods which demonstrated that the nucleic acid extraction efficiency of this cartridge system was slightly higher than that of the manual method.

Serum samples with HBV concentration of 5×10^5 IU/mL were used in this test. Four cartridges with 200 μL of samples re-

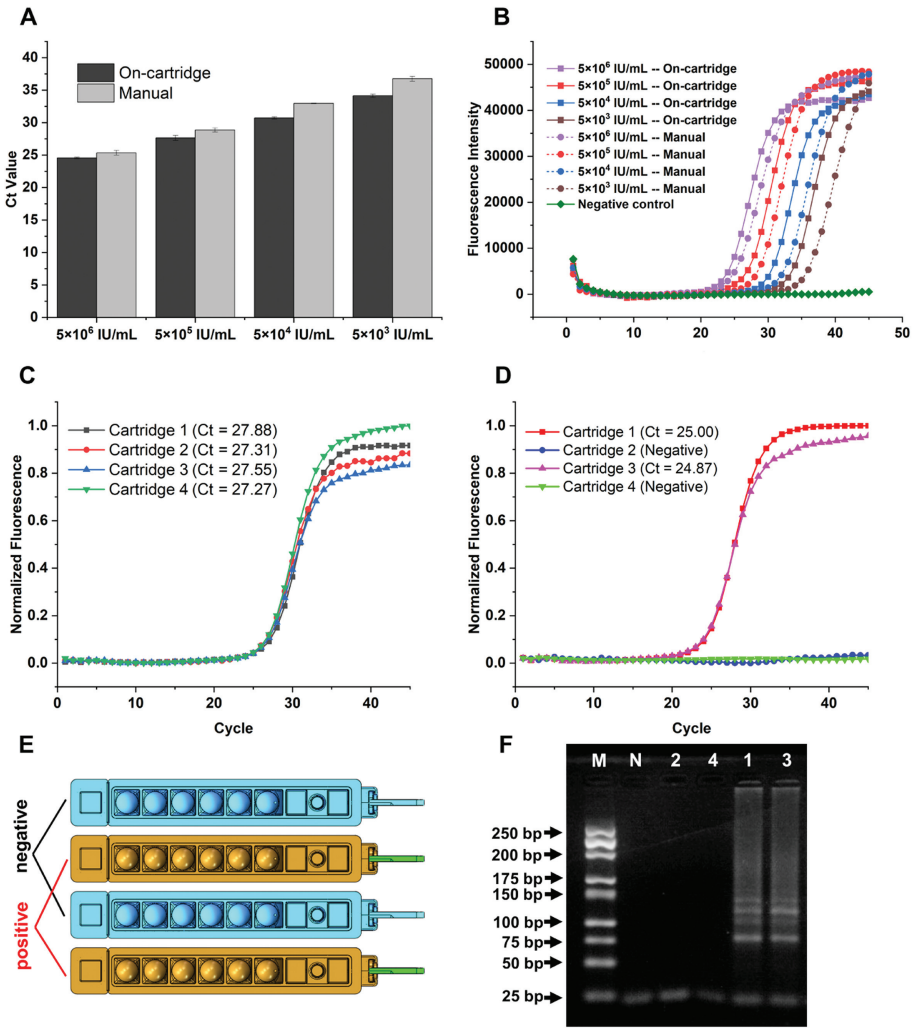

Fig. 3. (A) Average cycle threshold (Ct) values comparison HVB at the concentrations of 5×10^6 IU/mL, 5×10^5 IU/mL, 5×10^4 IU/mL and 5×10^3 IU/mL extracted by this cartridge system and by manual method respectively. (B) The real-time PCR fluorescence curves of these purified nucleic acid samples from StepOnePlus Real-time PCR System. (C) Real-time PCR fluorescence curves of the four channels cartridges with the calculated Ct values of 27.88, 27.31, 27.55 and 27.27. (D) Real-time PCR fluorescence curves of the four cartridges. (E) The cartridge setting for cross-contamination testing. (F) Electrophoretogram of the amplicons in cartridge 1 to cartridge 4. M represents the DNA marker, N represents the negative control without template.

spectively were loaded into the device for simultaneous NAD. Fig. 3C shows the fluorescence curves and their Ct values of the four channels with the coefficient of variation (CV) of 0.88%. The fluorescence curves and the calculated Ct values demonstrate the good uniformity of these four channels of the system.

For testing if there was cross-contamination between different cartridges when more than one cartridge was loaded in the device, positive serum samples with HBV at a concentration of 5×10^6 IU/mL and the negative control that without HBV were used. 200 μL of the positive samples were added to the cartridge 1 and 3, while the negative controls were added to cartridge 2 and 4 (Fig. 3E). Then, the four cartridges were loaded into the device for NAD, and the results of the test were analyzed (Fig. 3D). In addition, the amplicons of all cartridges were carefully pipetted out and evaluated by gel electrophoresis (Fig. 3F). The results demonstrated that there was no cross-contamination between different cartridges in a same detection processing.

To test the detection sensitivity of this cartridge system, the serum samples with 5×10^3 IU/mL of HBV were diluted with negative control serum samples to obtain three groups of samples with HBV at the concentrations of 5×10^2 IU/mL, 50 IU/mL, and 5 IU/mL. Combing with the negative control sample and the original samples of four concentrations (5×10^6 IU/mL, 5×10^5 IU/mL, 5×10^4 IU/mL, and 5×10^3 IU/mL), totally eight kinds of samples (200 μL of each) were divided into two groups for integrated NAD on this system. As shown in Figs. 4A and B, the LOD for HBV in serum samples by this cartridge system is about 5×10^2 IU/mL, which is close to the LOD (20 IU/mL) of the detection kit used in this paper.

In order to evaluate the multi-detection capability of this system, ORF1ab gene and N gene of SARS-CoV-2 were detected simultaneously on the homemade system. Here, we used nucleic acid releaser to release nucleic acids from SARS-CoV-2 without nucleic acid extraction step. The SARS-CoV-2 pseudoviruses at an original concentration of 2×10^8 copies/mL were diluted to 500 copies/mL by the nucleic acid releaser. Then, 45 μL of the above mixture was added to each cartridge that has been pre-loaded with lyophilized PCR reagent to carry out multiplex real-time RT-PCR. A total of 10 sets of parallel experiments were conducted, and Fig. 4C shows the real-time fluorescence curves of the results. Table 1 presents 10 sets of Ct values of the fluorescence curves. The results indicated that for SARS-CoV-2 with a concentration of 500 copies/mL 100% positive detection rate of both genes was achieved on our homemade cartridge system.

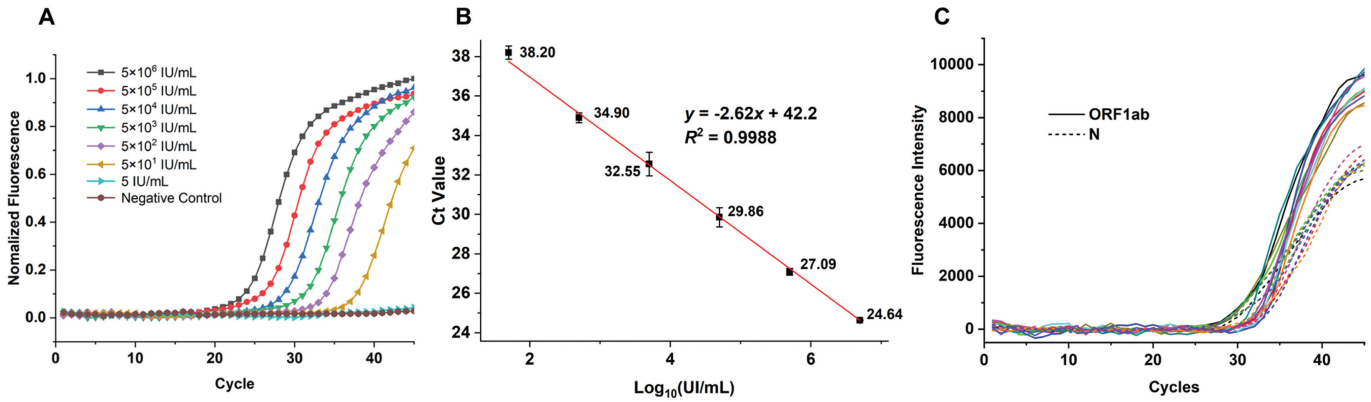

Fig. 4. The real-time RT-PCR fluorescence curves (A) and the standard curve (B) of the serum samples with HBV concentration of 5 IU/mL to 5×10^6 IU/mL. (C) The real-time fluorescence curves of ORF1ab gene and N gene of SARS-CoV-2 with the concentration of 500 copies/mL.

Table 1
10 sets of Ct values of ORF1ab gene and N gene of SARS-CoV-2.

Set#	Ct									
	1	2	3	4	5	6	7	8	9	10
ORF1ab	33.16	33.35	32.18	33.77	33.31	32.26	33.95	32.64	34.4	31.16
N	33.81	33.69	31.88	34.01	33.66	31.95	34.34	32.43	34.39	31.51

In this study, an integrated cartridge was developed for POC nucleic acid testing of infectious disease pathogens. Compared with the microfluidic chips, this cartridge has no complicated structure and does not require pumps to provide liquid driving force, but it is able to dispose up to 500 μL liquid samples, which can improve the detection sensitivity by enriching the target from large-volume samples. Performance evaluations results demonstrated that the designed cartridge was good at magnetic control and fluidic control, and on-cartridge NAE had better efficiency than manual extraction. In addition, the four cartridges in the device have good uniformity and there is no cross-contamination between them. Serum samples with HBV concentration of 5 IU/mL to 5×10^6 IU/mL were detected by the cartridge system. The LOD of this system for HBV in serum is 50 IU/mL. Finally, Multiplex detections of severe acute respiratory syndrome coronaviruses 2 (SARS-CoV-2) with a concentration of 500 copies/mL were carried out on the system and 100% positive detection rate was achieved.

In the following research, based on the current cartridge system, we will develop various kits for different detection methods, and conduct more NAD tests for different pathogen types and sample types.

Declaration of competing interest

The authors have no conflict of interest.

Acknowledgments

This research was financially supported by the National Natural Science Foundation of China (NSFC, No. 62071119), the Open Funding of State Key Laboratory of Oral Diseases (No. SKLOD2022OF05), the Jiangsu Provincial Key Research and Development Program (No. BA2020016) and the National Fund (No. BWS19C016).

Supplementary materials

Supplementary material associated with this article can be found, in the online version, at doi:10.1016/j.cclet.2022.108092.

References

[1] E. de Wit, N. van Doremalen, D. Falzarano, V.J. Munster, Nat. Rev. Microbiol. 14 (2016) 523–534.
[2] L. Baseler, D.S. Chertow, K.M. Johnson, H. Feldman, D.M. Morens, Annu. Rev. Pathol. 12 (2017) 387–418.
[3] D. Baud, D.J. Gubler, B. Schaub, M.C. Lanteri, D. Musso, Lancet 390 (2017) 2099–2109.
[4] R. Chilamakuri, S. Agarwal, Cells 10 (2021) 206.
[5] K. Dhama, S. Khan, R. Tiwari, et al., Clin. Microbiol. Rev. 33 (2020) e00028 20.
[6] W.S. Zhang, J. Pan, F. Li, et al., Anal. Chem. 93 (2021) 4126–4133.
[7] X. Zhu, X. Wang, L. Han, et al., Biosens. Bioelectron. 166 (2020) 112437.
[8] G.C.K. Mak, P.K.C. Cheng, S.S.Y. Lau, et al., J. Clin. Virol. 129 (2020) 104500.
[9] Z. Li, X. Ding, K. Yin, et al., Biosens. Bioelectron. 199 (2022) 113865.
[10] J.S. Park, K. Hsieh, L. Chen, et al., Adv. Sci. 8 (2021) 2003564.
[11] J.L. He, L. Luo, Z.D. Luo, et al., Resp. Med. 168 (2020) 105980.
[12] C. Long, H. Xu, Q. Shen, et al., Eur. J. Radiol. 126 (2020) 108961.
[13] M.L. Cunha, S.S. Da Silva, M.C. Stracke, et al., Anal. Chem. 94 (2022) 41–58.
[14] Z. Li, Y. Bai, M. You, et al., Biosens. Bioelectron. 177 (2021) 112952.
[15] M. Mauk, J. Song, C. Liu, H.H. Bau, Biosensors 8 (2018) 17.
[16] X. Wang, X.Z. Hong, Y.W. Li, et al., Mil. Med. Res. 9 (2022) 11.
[17] J. Yin, Y. Suo, Z. Zou, et al., Lab Chip 19 (2019) 2769–2785.
[18] Y. Xu, T. Wang, Z. Chen, et al., Chin. Chem. Lett. 32 (2021) 3675–3686.
[19] Z. Chen, T. Yang, H.W. Yang, et al., J. Biomed. Nanotechnol. 14 (2018) 198–205.
[20] E. Huang, Y. Wang, N. Yang, et al., Anal. Bioanal. Chem. 413 (2021) 1787–1798.
[21] N. Zong, Y. Gao, Y. Chen, X. Luo, X. Jiang, Anal. Chem. 94 (2022) 5196–5203.
[22] N. Li, Y. Lu, J. Cheng, Y. Xu, Lab Chip 20 (2020) 384–393.
[23] A.Y. Trick, H.T. Ngo, A.H. Nambiar, et al., Lab Chip 22 (2022) 945–953.
[24] Y.F. Zai, M. Chao, Z.L. Wang, et al., Lab Chip 22 (2022) 3436–3452.
[25] H. Chen, Y. Wu, Z. Chen, et al., J. Biomed. Nanotechnol. 13 (2017) 1619–1630.
[26] M. Hussain, Z. Chen, M. Lv, et al., Chin. Chem. Lett. 31 (2020) 3163–3167.
[27] X. Xu, N.Y. He, Chin. Chem. Lett. 32 (2021) 1747–1750.
[28] H. Chen, Y. Wu, Y. Fang, et al., Nanosci. Nanotechnol. Lett. 10 (2018) 1423–1428.
[29] H. Chen, Y.Q. Wu, Z. Chen, et al., Nanosci. Nanotechnol. Lett. 8 (2016) 1118–1126.
[30] Y.L. Fang, H.R. Liu, Y. Wang, et al., J. Biomed. Nanotechnol. 17 (2020) 407–415.
[31] M. Hussain, X.L. Liu, J. Zou, et al., Chin. Chem. Lett. 33 (2022) 1885–1888.
[32] H. Chen, X. Ma, X. Zhang, et al., Chin. Chem. Lett. 34 (2023) 107701.